

## Accepted Manuscript

This article can be cited before page numbers have been issued, to do this please use: K. R. M, S. R. K, N. T, B. B. Das, N. P. Lobo and K. V. Ramanathan, *New J. Chem.*, 2013, DOI: 10.1039/C3NJ00271C.



This is an *Accepted Manuscript*, which has been through the RSC Publishing peer review process and has been accepted for publication.

*Accepted Manuscripts* are published online shortly after acceptance, which is prior to technical editing, formatting and proof reading. This free service from RSC Publishing allows authors to make their results available to the community, in citable form, before publication of the edited article. This *Accepted Manuscript* will be replaced by the edited and formatted *Advance Article* as soon as this is available.

To cite this manuscript please use its permanent Digital Object Identifier (DOI®), which is identical for all formats of publication.

More information about *Accepted Manuscripts* can be found in the [Information for Authors](#).

Please note that technical editing may introduce minor changes to the text and/or graphics contained in the manuscript submitted by the author(s) which may alter content, and that the standard [Terms & Conditions](#) and the [ethical guidelines](#) that apply to the journal are still applicable. In no event shall the RSC be held responsible for any errors or omissions in these *Accepted Manuscript* manuscripts or any consequences arising from the use of any information contained in them.



Cite this: DOI: 10.1039/c0xx00000x

www.rsc.org/xxxxxx

ARTICLE TYPE

# $^{13}\text{C}$ - $^1\text{H}$ Dipolar couplings for probing rod-like hydrogen bonded mesogens

M. Kesava Reddy<sup>a</sup>, K. Subramanyam Reddy<sup>a</sup>, T. Narasimhaswamy<sup>b</sup>, Bibhuti B. Das<sup>c</sup>, Nitin P. Lobo<sup>d#</sup> and K.V. Ramanathan<sup>\*e</sup>

Received (in XXX, XXX) XthXXXXXXXXXX 20XX, Accepted Xth XXXXXXXXXXXX 20XX

DOI: 10.1039/b000000x

10 Hydrogen bonding is the most important non-covalent interaction utilised in building supramolecular assemblies and is preferred often as a means of construction of molecular, oligomeric as well as polymeric materials that show liquid crystalline property. In this work, a pyridine based nematogenic acceptor has been synthesized and mixed with non-mesogenic 4-methoxy benzoic acid to get a hydrogen bonded mesogen. The existence of hydrogen bonding between the pyridyl unit and the carboxylic acid  
15 was established using FT-IR spectroscopy from the observation of characteristic stretching vibrations of the unionized type at 2425 and 1927  $\text{cm}^{-1}$ . The mesogenic acceptor and the complex have been investigated using  $^{13}\text{C}$  NMR in solution, solid and liquid crystalline states. Together with the 2D separated local field NMR experiments, the studies confirm the molecular structure in the mesophase and yield the local orientational order parameters. It is observed that the insertion of 4-methoxy benzoic acid  
20 not only enhances the mesophase stability but also induces a smectic phase due to increase in the core length for the hydrogen bonded mesogen.

## Introduction

The properties of thermotropic liquid crystals in their mesophases depend on the nature of their constituent units namely, the central  
25 core which is fairly rigid and the flexible terminal chains. The core is constructed with either a linear or a non-linear chain of aromatic moieties connected by suitable linking units while either alkyl or alkoxy chains form the terminal units.<sup>1-3</sup> Depending upon the composition of the core, the intermolecular interactions differ  
30 resulting in a wide variety of mesophase morphologies.<sup>4,5</sup> For the construction of such mesogens, covalent linkages are usually preferred in view of their better stability.<sup>1-5</sup> By adopting this approach, a variety of mesogens with different molecular topologies have been synthesized and their mesophase properties  
35 characterized.<sup>6-8</sup> In recent years however, attention is also being paid to construction of mesogens involving non-covalent interactions. Among them, molecular designs that use hydrogen bonding have achieved a preeminent position.<sup>9-12</sup> In this strategy, the intermediates are usually constructed with covalent bonds and  
40 are classified as either donor or acceptor depending upon the kind of terminal functionality.<sup>9,10</sup> These are then allowed to interact through hydrogen bonding to produce new molecular systems. The H-bonded systems have the advantages of ease of construction and the possibility of modulating the interaction and

45 hence the mesophase property. Accordingly, molecular, macromolecular and supramolecular hydrogen bonded mesogens have been built with an excellent control on topology as well as on mesophase morphologies.<sup>13,14</sup> Thus there is considerable interest on the synthesis and the study of mesomorphic properties  
50 of hydrogen bonded liquid crystals.

The construction of materials with hydrogen bonding begins with the selection of a suitable donor and an acceptor. The mesogenic property can be introduced either in acceptor or donor moiety and literature enlists both kinds of systems.<sup>9-14</sup> For the purpose having  
55 a better control on the mesophase property, efforts in building hydrogen bonded mesogens have been directed towards the development of materials in which only one component is mesogenic and the other is non-mesogenic. In order to achieve liquid crystalline property in such mesogenic acceptor and non-  
60 mesogenic donor combinations, proper fine tuning of the molecular structure of the acceptor such as the length of the core is essential. In this scenario, the pyridine based acceptors have been generally favored and most often examined as mesogenic moieties with benzoic acids as donors.<sup>15,16</sup> One of the means  
65 obtaining detailed atomic level information of mesogenic molecules is the use of solid state NMR. However, only limited number of studies that utilize this technique to examine hydrogen bonded mesogens could be found in literature.<sup>17-19</sup> We present

here synthesis of a novel hydrogen bonded liquid crystalline system and a detailed investigation carried out using  $^{13}\text{C}$  NMR and other techniques.

In recent years, high resolution solid state  $^{13}\text{C}$  NMR studies have been used to obtain extensive atomic level information of several mesogenic systems. Both  $^{13}\text{C}$  chemical shifts and  $^{13}\text{C}$ - $^1\text{H}$  dipolar couplings have been utilized for this purpose.<sup>20-22</sup> The molecular order and relative orientations of different segments of the mesogens have been extracted employing this approach. In the present study, the molecular structure of a mesogenic acceptor and its hydrogen bonded mesogenic complex in solution, solid state and liquid crystalline phases have been examined using this approach. The mesogenic acceptor is constructed with three aromatic rings as the core with pyridine as one of the components while 4-methoxy benzoic acid is employed as the non-mesogenic donor. Along with  $^{13}\text{C}$  NMR, studies using hot stage optical microscopy (HOPM), differential scanning calorimetry (DSC) and FT-IR spectroscopy have been carried out to investigate both the acceptor and the complex. Studies of structurally simple hydrogen bonded mesogens like the one presented here could be expected to provide knowledge that can be used for understanding more complex systems that have been reported in literature in recent years.<sup>23-25</sup>

## Experimental Section

### Materials

4-pyridine carboxaldehyde, n-bromo hexane, N,N'-dicyclohexylcarbodiimide (DCC), 4-dimethylamino pyridine (DMAP) and 4-methoxy benzoic acid were purchased from Aldrich (USA) and used without further purification. Stannous chloride ( $\text{SnCl}_2$ ), N, N'-dimethylformamide (DMF), tetrahydrofuran (THF), triethylamine, ethanol and methanol (SD Fine Chemicals, Mumbai) were used as received. 4-hydroxy methyl benzoate, dichloromethane, ethyl acetate, diethyl ether, n-hexane, n-heptane, acetone, ethyl methyl ketone (EMK) and isopropanol were obtained from Merck (India) and used as received. 4-hexyloxy benzoic acid was synthesized in laboratory.

### Preparation of 4-[(E)-pyridin-4-ylmethylidene] amino} phenyl 4-hexyloxybenzoate (PMAH):

#### Synthesis of 4-hexyloxybenzoic acid (1,2)

#### 40 Synthesis of 4-hexyloxy methyl benzoate (1)

In a representative experiment, 4-hydroxy methyl benzoate (7.6 g, 0.05 mol) was placed in a 250 ml three necked round bottom flask equipped with stirrer and thermometer. To that, DMF (100 ml) and potassium carbonate (10.36 g, 0.075 mol) were added. The resulting mixture was stirred while maintaining the temperature at  $90^\circ\text{C}$ , then n-bromohexane (7.04 ml, 0.05 mol) was added through a pressure equalizing dropping funnel over a period of 30 minutes and the stirring was continued for about 4 hours and then the reaction mixture was allowed to cool to room temperature, poured into a two liter beaker.<sup>26</sup> The contents were diluted with water (150 ml) and then transferred to 250 ml separating funnel and diethyl ether was added. The ether layer collected was washed twice using 10% potassium hydroxide solution and followed by distilled water. Then the organic layer was dried over anhydrous sodium sulphate and upon evaporation of ether resulted in liquid 4-hexyloxy methyl benzoate.

#### Hydrolysis of 4-hexyloxy methyl benzoate (2)

4-hexyloxy methyl benzoate (9.45 g, 0.04 mol) was placed in 500 ml single neck round bottom flask equipped with double wall water condenser. Ethanol (150 ml) and potassium hydroxide (6 g, 0.1 mol) dissolved in distilled water (150 ml) were added to the flask. The solution was refluxed for two hours and allowed to cool to room temperature and neutralized with 10% hydrochloric acid to get a white precipitate.<sup>26</sup> The compound was purified by recrystallizing from methanol.

#### 4-hexyloxy benzoic acid (2)

Yield: 84.7%, m.p- $112^\circ\text{C}$ , FT-IR (KBr,  $\text{cm}^{-1}$ ): 2941, 2867 ( $\text{C}-\text{H}_{\text{str}}$ ), 2549 ( $\text{O}-\text{H}_{\text{str}}$  of carboxylic acid), 1683 ( $\text{C}=\text{O}_{\text{str}}$  of carboxylic acid), 1604, 1511 ( $\text{C}=\text{C}_{\text{str}}$  aromatic), 1467, 1426 ( $\text{C}-\text{H}_{\text{ben}}$ ) 1297, 1253, 1166, 1121, ( $\text{C}-\text{O}-\text{C}_{\text{asym\&symstr}}$  of ether);  $^1\text{H}$ -NMR ppm ( $\text{CDCl}_3$ ): 8.8.06 (d, 2H), 6.93 (d, 2H), 4.01 (t, 2H), 1.78 (m, 2H), 1.46 (m, 2H), 1.33 (t, 4H), 0.90 (t, 3H);  $^{13}\text{C}$ -NMR ppm ( $\text{CDCl}_3$ ): 8172.38, 163.79, 132.43, 121.48, 114.26, 68.37, 31.64, 29.15, 25.76, 22.69 and 14.13.

#### 75 Synthesis of 4-aminophenyl 4-hexyloxybenzoate (3,4)

#### Synthesis of 4-nitrophenyl 4-(hexyloxy) benzoate (3)

In a representative experiment, 4-hexyloxy benzoic acid (5 g, 0.02 mol) and 4-nitro phenol (2.78 g, 0.02 mol) were placed in a conical flask. To this, dichloromethane (100 ml) was added and the solution was stirred at room temperature with magnetic stirrer. 4-Dimethylamino pyridine (0.24 g, 0.002 mol) was added as a catalyst to the solution. After 10 minutes, DCC (5.15 g, 0.025 mol) dissolved in dichloromethane was added to the flask and the solution was allowed to stir for 12 hrs. The precipitated N,N'-dicyclohexyl urea was filtered off and washed with excess of dichloromethane (100 ml). The combined organic solution was taken into separating funnel and then washed twice with 5% KOH solution followed by distilled water. The yellow solid obtained was purified by recrystallization from isopropyl alcohol.

#### 90 4-nitrophenyl 4-(hexyloxy) benzoate (3)

Yield: 72.4%, m.p- $68^\circ\text{C}$ , FT-IR (KBr,  $\text{cm}^{-1}$ ): 2934, 2865 ( $\text{C}-\text{H}_{\text{str}}$ ), 1742 ( $\text{C}=\text{O}_{\text{str}}$ ), 1605 and 1516 ( $\text{C}=\text{C}_{\text{str}}$  aromatic), 1487, 1319 ( $\text{C}-\text{H}_{\text{ben}}$ ), 1343 ( $-\text{NO}_2_{\text{str}}$ ), 1255, 1164 ( $\text{C}-\text{O}-\text{C}_{\text{asym\&symstr}}$  of ester and ether);  $^1\text{H}$ -NMR ppm ( $\text{CDCl}_3$ ): 8.8.28 (d, 2H), 8.12 (d, 2H), 7.39 (d, 2H), 6.98 (d, 2H), 4.03 (t, 2H), 1.86 (m, 2H), 1.47 (m, 2H), 1.34 (m, 4H), 0.90 (t, 3H);  $^{13}\text{C}$ -NMR ppm ( $\text{CDCl}_3$ ): 8164.14, 164.03, 156.06, 145.26, 132.59, 125.27, 122.76, 120.40, 114.59, 68.53, 31.63, 29.12, 25.74, 22.69 and 14.13.

#### Reduction of 4-nitrophenyl 4-(hexyloxy) benzoate (4)

In this experiment, 4-nitrophenyl 4-(hexyloxy) benzoate (3.21 g, 0.00936 mol) and  $\text{SnCl}_2$  (10.53 g, 0.046 mol) were placed in a single necked round bottom flask along with ethanol and refluxed for two hrs.<sup>28</sup> Then it was cooled to room temperature, neutralized with 10%  $\text{NaHCO}_3$  solution then filtered and solid obtained was dried in vacuum oven. The solid was treated with 100 ml EMK for 1 hr and the solvent was evaporated to get light brown solid which was recrystallized from heptane.

#### 4-aminophenyl 4-hexyloxybenzoate (4)

Yield: 76.1%, m.p- $91^\circ\text{C}$ , FT-IR (KBr,  $\text{cm}^{-1}$ ): 3407, 3329 ( $\text{NH}_{2\text{str}}$ ), 3212 (aromatic  $\text{C}-\text{H}_{\text{str}}$ ), 2934, 2861 ( $\text{C}-\text{H}_{\text{str}}$ ), 1721 ( $\text{C}=\text{O}_{\text{str}}$ ), 1607, 1512 ( $\text{C}=\text{C}_{\text{str}}$  aromatic), 1467, 1420, 1395 and 1315 ( $\text{C}-\text{H}_{\text{ben}}$ ), 1261, 1196, 1166 ( $\text{C}-\text{O}-\text{C}_{\text{asym\&symstr}}$  of ester and ether);  $^1\text{H}$ -NMR ppm ( $\text{CDCl}_3$ ): 8.8.13 (d, 2H), 6.96 (m, 4H), 6.69 (d, 2H), 4.03 (t, 2H), 3.54 (s, 2H), 1.81 (m, 2H), 1.47 (m, 2H), 1.35 (m, 4H), 0.92 (t, 3H);  $^{13}\text{C}$ -NMR ppm ( $\text{CDCl}_3$ ): 8165.68,

163.47, 144.31, 143.21, 132.28, 122.46, 121.88, 115.80, 114.31, 68.38, 31.66, 29.17, 25.77, 22.72 and 14.18.

#### Synthesis of 4-[(E)-pyridin-4-ylmethylidene] amino} phenyl 4-hexyloxybenzoate (PMAFH) (5)

5 In a representative experiment, 4-aminophenyl 4-hexyloxy benzoate (0.939 g, 0.003 mol) and 4-pyridine carboxaldehyde (0.32 g, 0.003 mol) in equimolar were taken in a 100 ml conical flask. Few drops of ethanol were added and the flask was placed in a microwave oven (power: 40 W) for ten minutes. Then it was

10 allowed to cool to room temperature, washed with methanol and recrystallized twice from heptane.  
Yield: 71.2 %, m.p-105.0 °C, FT-IR (KBr, cm<sup>-1</sup>): 3063 (aromatic C-H<sub>str</sub>), 2927, 2864 (C-H<sub>str</sub>), 1726 (C=O<sub>str</sub>), 1603, 1507 (C=C<sub>str</sub> aromatic), 1466, 1416, 1318 (C-H<sub>ben</sub>), 1263, 1198, 1167 (C-O-C<sub>asym&symstr</sub> of ester and ether); <sup>1</sup>H-NMR ppm (CDCl<sub>3</sub>): 8.76 (d, 2H), 8.48 (s, 1H), 8.15 (d, 2H), 7.77 (d, 2H), 7.30 (m, 4H), 6.97 (d, 2H), 4.03 (t, 2H), 1.83 (m, 2H), 1.47 (m, 2H), 1.35 (m, 4H), 0.91 (t, 3H); <sup>13</sup>C-NMR ppm (CDCl<sub>3</sub>): 151.90, 150.62, 150.13, 148.39, 142.78, 132.34, 122.67, 122.29, 122.0, 121.39, 114.39, 114.39, 68.39, 31.57, 29.09, 25.68, 22.61 and 14.04.

#### Synthesis of hydrogen bonding complex:

#### [4-[(E)-pyridin-4-ylmethylidene] amino} phenyl 4-hexyloxybenzoate and 4-methoxy benzoic acid] (PMAFHMB) (6)

25 In an experiment, 4-[(E)-pyridin-4-ylmethylidene] amino} phenyl 4-hexyloxybenzoate (1.3 g, 0.0032 mol) and 4-methoxy benzoic acid (0.33 g, 0.0032 mol) were placed in 100 ml conical flask kept on magnetic stirrer and THF (15 ml) was added.<sup>29</sup> The

30 reaction mixture was stirred for about one hour and after that poured into evaporating bowl and solvent was allowed to evaporate slowly at room temperature. The solid obtained was recrystallized twice from heptane.  
Yield: 69.3%, m.p-101 °C, FT-IR (KBr, cm<sup>-1</sup>): 2948, 2865 (C-H<sub>str</sub>), 2425 (OH<sub>str</sub>-H Bond) 1710 (C=O<sub>str</sub>), 1605, 1511 (C=C<sub>str</sub> aromatic), 1471, 1417(C-H<sub>ben</sub>), 1255, 1166, 1197 (C-O-C<sub>asym&symstr</sub> of ester and ether); <sup>1</sup>H-NMR ppm (CDCl<sub>3</sub>): 8.79 (d, 2H), 8.49 (s, 1H), 8.16 (d, 2H), 8.08 (d, 2H), 7.80 (d, 2H), 7.30 (m, 4H), 6.97 (m, 4H), 4.05 (t, 2H), 3.88 (s, 3H), 1.83 (m, 2H), 1.49 (m, 2H), 1.37 (m, 4H), 0.92 (t, 3H); <sup>13</sup>C-NMR ppm (CDCl<sub>3</sub>): 151.90, 150.62, 150.13, 148.39, 142.78, 132.34, 132.28, 122.68, 122.44, 122.07, 122.02, 121.38, 114.39, 113.73, 68.40, 55.48, 31.57, 29.09, 25.68, 22.61 and 14.03.

#### Instrumental details

45 FT-IR spectra of all the compounds were recorded on an ABB BOMEM MB3000 spectrometer using KBr pellets. <sup>1</sup>H and <sup>13</sup>C NMR spectra of the compounds in CDCl<sub>3</sub> were run on a JEOL 500 MHz instrument at room temperature using tetramethylsilane as an internal standard. The resonance frequencies of <sup>1</sup>H and <sup>13</sup>C were 500.15 and 125.76 MHz respectively. The nature of the mesophase and the temperature of occurrence of various phases were determined with an Olympus BX50 polarizing optical microscope equipped with a Linkam THMS 600 stage with a TMS 94 temperature controller. The photographs were taken

55 using an Olympus C7070 digital camera. Differential scanning calorimetry (DSC) traces were recorded using a DSC Q200 instrument with a heating rate of 10°C/minute in nitrogen atmosphere.

#### Solid state NMR measurements

60 Solid-state NMR experiments were carried out on the samples using a BrukerAvance-III 500 WB NMR spectrometer. The proton and carbon resonance frequencies were 500.17 and 125.79 MHz respectively. The spectra in the liquid crystalline phases of the samples were obtained using a double resonance probe equipped with a 5 mm solenoid coil for static samples using the Hartmann-Hahn cross-polarization pulse sequence with a contact time of 2ms following the 90° proton pulse of width of 4 μs. SPINAL-64<sup>30</sup> decoupling was employed during carbon signal acquisition using a proton decoupling power of 30 kHz. To avoid

70 sample heating, the recycle delay between each FID was kept as 8s. Each spectrum was obtained typically with 256 scans. For measuring the <sup>13</sup>C-<sup>1</sup>H dipolar couplings of the molecules in their mesophase, the SAMPI4 pulse sequence (given in ESI) was applied on the oriented sample under static conditions.<sup>31</sup> Details

75 of the application of the pulse sequence to liquid crystalline systems have been described in earlier publications<sup>32,33</sup> and in caption of Figure 1 in ESI. The method yields a 2D spectrum with carbon chemical shifts along the direct dimension and the proton-carbon dipolar coupling frequencies along the indirect dimension.

80

## Results and Discussion

#### FT-IR and Mesophase characterization

The molecular structures of the mesogenic acceptor PMAFH and 85 the hydrogen bonded mesogen PMAFHMB are shown in Figure 1A&B. As described in the experimental section, the mesogenic acceptor was synthesized from 4-hexyloxy benzoyloxy aniline<sup>34</sup> by reacting it with 4-pyridine carboxaldehyde in ethanol (Scheme-1). Lee et al. reported the mesophase properties of some 90 of the homologues of the mesogenic acceptor.<sup>16</sup> The hydrogen bonded complex is prepared by mixing equimolar ratio of mesogenic pyridine and non-mesogenic acid in THF (Scheme-1). The structural confirmation of the mesogenic acceptor and its complex with 4-methoxy benzoic acid has been accomplished by 95 FT-IR and solution NMR (<sup>1</sup>H and <sup>13</sup>C) techniques. For the hydrogen bonded complex, in addition to 1D solution NMR, 2D experiments such as <sup>1</sup>H-<sup>1</sup>H DQF COSY and <sup>13</sup>C-<sup>1</sup>H HSQC were also carried out for spectral assignment. The existence of hydrogen bond in the mixture of acceptor and donor is 100 established by FT-IR spectroscopy. The FT-IR spectra of 4-methoxy benzoic acid, PMAFH and their hydrogen bonded complex are shown in ESI. The FT-IR spectrum of PMAFH (ESI) shows the following characteristic absorption frequencies : C-H stretching at 2927 and 2864 cm<sup>-1</sup>, ester carbonyl stretching at 105 1726 cm<sup>-1</sup>, ring skeletal (C=C) vibrations at 1603 and 1507 cm<sup>-1</sup> and C-O-C stretching at 1263 and 1167 cm<sup>-1</sup>. For the case of 4-methoxy benzoic acid, the O-H stretching frequencies of carboxylic acid are seen at 2669 and 2557 cm<sup>-1</sup> which are considered to be due to Fermi resonances.<sup>35,36</sup> The carbonyl 110 stretching absorption band of carboxyl acid (donor) is noticed at 1686 cm<sup>-1</sup> due to dimerization induced by intermolecular hydrogen bonding. In the case of the mesogenic complex, disappearance of the bands at 2669 and 2557 cm<sup>-1</sup> which are noticed for 4-methoxy benzoic acid (ESI) and appearance of two 115 new bands at 2425 and 1927 cm<sup>-1</sup> (ESI) confirms the hydrogen bonding between acceptor and donor.<sup>37,38</sup> These two new bands

are strong evidence of the intermolecular hydrogen bonding of the unionized type between the pyridyl unit and the carboxylic acid.<sup>37,38</sup> Further, an increase in carbonyl stretching vibration of acid component is clearly noticed. Thus, the C=O stretching of carboxyl carbonyl of 4-methoxy acid is seen at 1686 cm<sup>-1</sup> whereas in the hydrogen bonded complex the value shifts and appears at 1704 cm<sup>-1</sup>. The increase in C=O stretching of acid group is the result of the intermolecular hydrogen bonds.<sup>39</sup> Further evidence for the formation of the complex is available from the NMR studies of the mesophase.

The mesophase transition temperatures of the acceptor and the hydrogen bonded mesogen have been determined by HOPM and DSC methods. For PMAPH, DSC studies reveal a crystal to nematic phase (Cr-N) transition at 105.0 °C and a transition from the nematic to isotropic phase (N-I) at 152.1 °C with the transition enthalpy values being 3.56 and 0.08 K.cal/mole respectively for the two transitions (ESI). In HOPM studies, the sample upon cooling from isotropic phase showed birefringent droplets which on further cooling transformed to a homeotropic texture confirming the occurrence of the nematic phase. The hydrogen bonded complex (PMAPHMB), on the other hand, showed smectic A (S<sub>A</sub>) phase (Figure 2) in addition to nematic phase. Accordingly, in DSC, a Cr-S<sub>A</sub> transition is noticed at 101.2 °C. S<sub>A</sub>-N transition occurs at 121.0 °C and the N-I transition is observed at 200.7 °C. The transition enthalpies are found to be 9.77, 0.01 and 0.63 K.cal/mole for the three transitions respectively (ESI). In HOPM studies, the sample on cooling the isotropic phase, showed birefringent droplets which coalesced to give homeotropy. On further cooling, N-S<sub>A</sub> phase transition is noticed. Interestingly, the homeotropy persisted in the smectic A phase also. However, some areas of the sample showed birefringent polygonal texture characteristic of smectic A phase.<sup>40</sup> Thus, the HOPM and DSC data unambiguously support the existence of mesophase both in the acceptor as well as in the hydrogen bonded complex. Since 4-methoxy benzoic acid is non-mesogenic, it showed a single phase transition corresponding to the Cr-I transition at 185 °C.<sup>40</sup> It is thus interesting to note that the H-bonded complex has more number of phases as well as wider mesophasic temperature range, exhibiting better mesophase stability.

#### <sup>13</sup>C NMR Investigations of PMAPH

<sup>13</sup>C NMR studies of the mesogenic donor and its hydrogen bonded complex were carried out in solution, solid phase and nematic phase with a view to examine the molecular structure. In nematic phase, in addition to static 1D experiments, 2D SLF experiments are carried out to find the <sup>13</sup>C-<sup>1</sup>H dipolar couplings of the phenyl rings and imine units to determine the order parameter of the core unit.

#### In solution state

The proton decoupled <sup>13</sup>C NMR spectrum of PMAPH in CDCl<sub>3</sub> recorded at room temperature is shown in Figure 3A. The spectrum shows well resolved lines with varying intensities at different chemical shift values for core as well as terminal chain carbons. The individual assignment of signals was carried out by iterating the spectrum by the ACD/chemsketch software. For the core unit carbons, the lines are observed in the range 114-165 ppm. The mesogen has two phenyl rings and one pyridine ring and as a result six methine carbon signals are expected in the

range 114-151 ppm. The interesting feature of the spectrum is appearance of one of the phenyl methine carbons at 150.6 ppm due to the presence of nitrogen of pyridine ring adjacent to it. The characteristic imine carbon is noticed at 157.9 ppm. The quaternary carbons accounting for the entire core unit are well resolved and the chemical shifts of all core unit carbons are listed in Table 1. The hexyloxy chain shows six sharp lines among which OCH<sub>2</sub> carbon is seen distinctly at 68.3 ppm. The other methylene and terminal methyl carbon signals are noticed in the range 22-32 ppm and 14.0 ppm respectively.

#### Spectrum in the solid state

<sup>13</sup>C CP-TOSS spectrum<sup>41</sup> of the mesogen in the solid phase at room temperature is shown in Figure 3B. The spectrum shows relatively broad peaks in contrast to solution spectrum. Also more peaks compared to solution are observed in the solid state. In solution, for the core unit carbons, 13 peaks are noticed whereas in the solid state, 21 peaks are observed. The additional peaks are noticed for both the methine and the quaternary carbons of the core unit. Similar observations have been made for other mesogenic molecules in the solid state.<sup>20,32</sup> The reasons for the appearance of multiple lines in the solid state are many. The freezing of the flip motion about the para-axis of the benzene ring has been observed to result in additional lines for the core unit carbons.<sup>32</sup> In this case, the degeneracy of the methine carbon resonances in the three ring units of the core is removed and six more carbon peaks are expected. Other reasons include the presence of more than one molecule in the unit cell or the presence multiple conformers. In the present case, additional peaks are observed both in the region of the aromatic CH carbons and in the region of the quaternary carbons indicating that the peaks arise from molecules differing in their structure or environment. Additional peaks are not seen in the hexyloxy chain region in the present case. This can be attributed to the relatively smaller span of the chemical shift anisotropy of the aliphatic carbons and the larger line width of the spectra in the solid state.

#### Spectrum in the mesophase

The mesogen exhibits an enantiotropic nematic phase in the range 105.0-152.1 °C. The <sup>13</sup>C NMR spectrum of the mesogen was acquired at several temperatures while heating the sample in the magnetic field. Well resolved sharp intense peaks were noticed in the mesophase. A typical spectrum obtained at 125 °C is shown in Figure 3C. As seen in the spectrum, the chemical shift values of all the carbons in the mesophase are different compared to those observed in the solution spectrum. For the assignment of the spectrum in the mesophase, the following procedure was used. The spectrum shows five sharp intense peaks in the region 135-170 ppm. Based on their intensities and also from the dipolar splitting in the 2D-NMR spectrum discussed subsequently, these peaks are assigned to the six non-equivalent methine carbons in the three methyl rings of the core unit of the mesogen. Among them, the peak appearing at 148.6 ppm and showing the highest intensity corresponds to overlapped resonances of two phenyl ring methine carbons. For the assignment of chemical shifts of the carbons of ring I, the similarity of ring I to alkoxy benzoic acids has been utilized. The alkoxy benzoic acids are important class of mesogens and are often used as core components for a wide range of mesogens. Among them three mesogens which share the 4-alkoxy benzoic acid as a first ring have been

considered for comparing the chemical shift trends in their respective mesophases. For instance, in the case of 10B1M7 and HZL7 Dong et al.<sup>42</sup> and Domenici et al.<sup>43</sup> used decyloxy and heptyloxy benzoic acids for the construction of respective mesogens. Similarly, the hockey-stick mesogen reported in literature<sup>44</sup> is constructed with decyloxy benzoic acid. In all the cases, the <sup>13</sup>C NMR data is available in their mesophase. Though these mesogens exhibit smectic phases at different mesophase temperatures, the pattern of peak appearance and its trend particularly for the 4-alkoxy benzoic acid unit, facilitated the assignment of ring carbons. In the case of the carbon of the azomethine connecting unit, the peak is easily identified at 195.8 ppm from the large dipolar splitting observed in the 2D NMR spectrum. For the rest of the aromatic carbons, the trend observed in the solution NMR spectrum has been utilized and the peaks assigned. In addition, the <sup>13</sup>C spectra have also been recorded as a function of temperature and the chemical shifts are shown as a function of temperature in Figure 4A. The figure shows nearly uniform variation of the aromatic carbon chemical shifts as a function of temperature. For the terminal hexyloxy chain, similar to solution spectrum, six peaks are observed. The increase of chemical shift values of core unit carbons and marginal decrease for hexyloxy chain carbons in contrast to solution spectrum is indicative of the parallel alignment of the molecules in the magnetic field.<sup>45,46</sup> The assigned chemical shift values of all the carbons of the core unit of the aligned spectrum are listed in Table 1.

#### 2D-SLF study in the mesophase

The 2D-SAMPI4 NMR spectrum of the mesogen recorded at 125 °C is shown in Figure 5A. The well resolved contours in the 2D spectrum provide both <sup>13</sup>C chemical shifts as well as <sup>13</sup>C-<sup>1</sup>H dipolar couplings. The 2D data is thus useful both for confirming the 1D assignment and also for determining the orientational order parameters. The spectrum in the region 132-200 ppm shows 7 intense contours arising from CH vectors of the core unit among which 6 are assigned to CH carbons of phenyl as well as pyridine rings. In 1D static spectrum, the peak appearing at 149.4 ppm was assigned to two carbons. In the 2D spectrum the appearance of a correspondingly intense and broad contour is indicative of two carbons with slightly different dipolar couplings and confirms the 1D assignment. The azomethine carbon is seen distinctly due to its attached proton resulting in a large value for the <sup>13</sup>C-<sup>1</sup>H dipolar coupling. The quaternary carbons of the core unit also showed contours due to long range coupling with neighboring CH carbons. For the terminal hexyloxy chain, the 2D spectrum showed five contours with varying <sup>13</sup>C-<sup>1</sup>H dipolar couplings. Table 1 lists the <sup>13</sup>C-<sup>1</sup>H dipolar couplings of all the resolved core unit carbons of the mesogen.

#### <sup>13</sup>C NMR Investigations of PMAPHMB

##### In solution state

The molecular structure of the mesogen along with carbon numbering is shown in Figure 1B. The proton decoupled <sup>13</sup>C NMR of hydrogen bonded mesogen was recorded at room temperature in CDCl<sub>3</sub>. The spectrum (Figure 6A) shows well resolved lines and the assignment of the signals was carried out using the ACD chemsketch software and further confirmed by <sup>1</sup>H-<sup>1</sup>H DQF and <sup>13</sup>C-<sup>1</sup>H HSQC experiments (vide ESI). With the incorporation of 4-methoxy benzoic acid, an additional set of five

peaks at 170.6, 163.8, 132.3, 122.4 and 113.7 ppm in the aromatic region and a peak corresponding to the methoxy carbon at 55.4 ppm are observed. Table 2 lists the chemical shift values along with peak assignments. Thus, 18 lines seen in the aromatic part of the spectrum account for both donor and acceptor in the hydrogen bonded mesogen.

##### Spectrum in the solid state

The <sup>13</sup>C CP-TOSS NMR spectrum of the complex in the solid state is shown in Figure 6B. As in the case of the spectrum of the acceptor, the solid state spectrum shows, in comparison to the spectrum in the solution state, several additional peaks in the aromatic range of 117-169 ppm as well as in the aliphatic range of 10-34 ppm. The spectral features corresponding to the donor and acceptor moieties in the complex are easily distinguished. Thus, the characteristic methoxy carbon at 55.9 ppm and the ester carbonyl at 169.4 ppm indicate the presence of 4-methoxy benzoic acid unit in the hydrogen bonded mesogen. Many of the peaks in the solid state can be identified from comparison to spectra in the solution phase. However, such assignments are tentative in the absence of other experimental evidence and hence are not listed.

##### Spectrum in the mesophase

The hydrogen bonded complex (PMAPHMB) shows mesophase in the range 101.2-200.7 °C. It exhibits both smectic A and nematic phases. The Cr-S<sub>A</sub> transition is observed at 101.2 °C while S<sub>A</sub>-N transition is noticed at 121 °C. The spectrum of the static sample in the nematic phase was obtained over a range of temperatures and the spectrum obtained at 130 °C is shown in Figure 6C. The spectral features correspond to a parallel alignment of the molecule in the magnetic field. The key feature of the spectrum is the appearance of eight sharp peaks in the range 140-170 ppm in comparison to that of PMAPH where six peaks accounting for three rings in the core are only noticed. The additional lines belong to the methoxy benzoic acid unit. These lines are shifted towards the higher frequency range of the spectrum in comparison to the spectral lines in the isotropic phase and with an alignment induced shift very similar to the carbons of the phenyl rings of the acceptor. In addition, as discussed in the subsequent section, the <sup>13</sup>C-<sup>1</sup>H dipolar couplings for the methine carbons of both the donor and acceptor moieties in the complex are very similar. In a similar fashion, the methoxy carbon peak of the donor is shifted towards the lower frequency range in the mesophase in a manner similar to the oxymethylene carbon of the acceptor part. These observations are conclusive proof of the fact that the benzoic acid unit is a part of the complex. The detailed spectral assignment of PMAPHMB mesogen has been carried out in a manner similar to the one adopted for the case of the spectrum of PMAPH. Among the peaks noticed for PMAPHMB mesogen, the azomethine carbon is seen at 205.9 ppm while the characteristic ester carbonyl is noticed at 214.7 ppm. Table 2 lists the <sup>13</sup>C chemical shift assignment of all the carbons of PMAPHMB along with alignment induced chemical shifts. In this case also, the spectra were recorded at different temperatures and the plot shown in Figure 4B, enables following the variation of the <sup>13</sup>C chemical shift as a function of temperature.

##### 2D SLF Spectrum

The SAMPI4 pulse sequence was applied on the sample and the 2D-SLF spectrum in the nematic phase was obtained at 130 °C.

The spectrum (Figure 5B) shows well resolved dipolar cross-peaks for all the carbons. A visual inspection of the cross-sections of the different carbons provides additional support for the assignment of the 1D spectrum. For instance, eight well separated contours for the aromatic CH vectors are distinctly seen. Similarly, the azomethine CH showed contour at 205.9 ppm with high  $^{13}\text{C}$ - $^1\text{H}$  dipolar coupling value (5.14 kHz). On the other hand, the quaternary carbons show very small separation. For the terminal carbons, the characteristic  $\text{OCH}_2$  of hexyloxy chain and  $\text{OCH}_3$  of the 4-methoxybenzoic acid fragment showed distinctly different dipolar coupling values making their identification simpler. Table 2 lists the  $^{13}\text{C}$ - $^1\text{H}$  dipolar coupling values of all the core unit carbons of acceptor and donor units. The 2D data in addition to providing confirmation of the spectral assignment can also be used to obtain the local order parameters of the different structural units. This is presented in the next section for the aromatic core units of both the acceptor and the complex.

### Orientalional order parameters

The  $^{13}\text{C}$  NMR data of PMAPH and PMAPHMB mesogens can be used for calculating the orientational order parameters in their nematic phases. The 2D-SAMPI4 experiment is an improved version of the PISEMA experiment<sup>47</sup> and from the dipolar oscillation frequencies obtained from the experiment, the local order parameters  $S'_{zz}$  and  $S'_{xx} - S'_{yy}$  of the phenyl rings can be derived as follows.<sup>32,48</sup> In the case of the methine carbons of the phenyl ring, the experimental dipolar frequency has two contributions namely a coupling to the attached proton  $D_{\text{C-Hi}}$  and also a coupling to the remote proton at the *ortho* position  $D_{\text{C-Ho}}$ . The measured frequency is given by<sup>49</sup>  $[(D_{\text{C-Hi}})^2 + (D_{\text{C-Ho}})^2]^{1/2}$ . The quaternary carbons do not have an attached proton, but have couplings to two equivalent protons at the *ortho* positions. In this case the dipolar frequency is  $\sqrt{2} * (D_{\text{C-Ho}})$ . The dipolar couplings are related to the local order parameters and are given by the equation<sup>21b, 45</sup>

$$D_{\text{C-H}} = K \left\{ \frac{1}{2} (3 \cos^2 \theta_z - 1) S'_{zz} + \frac{1}{2} (\cos^2 \theta_x - \cos^2 \theta_y) (S'_{xx} - S'_{yy}) \right\} \quad (1)$$

where  $K = -h\gamma_{\text{C}}\gamma_{\text{H}}/4\pi^2 r_{\text{CH}}^3$  in which  $\gamma_{\text{C}}$  and  $\gamma_{\text{H}}$  are gyromagnetic ratios of carbon and hydrogen nuclei respectively,  $r_{\text{C-H}}$  is the distance between the nuclei C and H and  $\theta_x$ ,  $\theta_y$  and  $\theta_z$  the angles the C-H vector makes with the coordinate axes. Here, the z, x and y-axes are defined to be respectively the para axis of the phenyl ring, an axis perpendicular to the z axis but in the plane of the ring and the axis perpendicular to the plane of the ring. Using the above expression, the local order parameters  $S'_{zz}$  and  $S'_{xx} - S'_{yy}$  can be calculated from the experimentally determined dipolar frequencies for each of the phenyl rings. For calculating K in eq.1, standard bond distances, namely 1.09 Å for the C-H bond and 1.4 Å for the C-C bond have been assumed. For the CCH bond angle, in view of the uncertainty in the position of the H atom as determined by X-rays, it has been found necessary to vary the two C-C-H bond angles, which are found to deviate slightly from the value of 120° expected for an ideal hexagonal geometry.<sup>48,50</sup> Accordingly, in the fitting procedure, the two C-C-H bond angles have also been slightly varied around 120°. Table 3 lists the local order parameters thus obtained for each phenyl ring of both the mesogens in their nematic phases. The variation of the chemical shifts shown as a function of temperature in Figure 4 for PMAPH and PMAPHMB can also be utilized for

calculating the order parameters.<sup>42,51,52</sup> However, this requires a knowledge of the chemical shift anisotropy (CSA) tensor values. Based on the similarity of ring I of both PMAPH and PMAPHMB to the phenyl ring of 4-hexyloxy benzoic acid (HBA), we have utilized the CSA tensor values available for HBA in literature<sup>32</sup> and have determined the order parameters of ring I at different temperatures as follows. The alignment induced chemical shift ( $\delta_{\text{lc}}$ ) in the liquid crystalline phase to that in the solution phase ( $\delta_{\text{soln}}$ ) is related to the components of the chemical shift tensor  $\delta_{ij}$  and the local order parameters  $S'_{zz}$  and  $(S'_{xx} - S'_{yy})$  of the phenyl ring according to,<sup>21b</sup>

$$\delta_{\text{lc}} - \delta_{\text{soln}} = (2/3) S'_{zz} [P_2(\cos\beta)(\delta_{11} - \delta_{22}) + (1/2)(\delta_{22} - \delta_{33})] + (1/3) (S'_{xx} - S'_{yy}) [ \delta_{33} - (\cos^2\beta)\delta_{22} - (\sin^2\beta)\delta_{11} ] \quad (2)$$

Here again, the z-axis is the para-axis of the ring, the x-axis is in the plane of the ring and the y-axis is perpendicular to the plane.

The angle  $\beta$  is the angle between the component  $\delta_{11}$  of the chemical shift tensor and the z-axis and is taken as 0° and 60° for carbons in the *para* the *ortho* positions respectively. The obtained order parameters for ring I are shown as a function of temperature in Figure 7 for both PMAPH and PMAPHMB. It is noticed that the values of order parameters obtained from using the dipolar couplings given in Table 3 compare well with the values obtained using the chemical shifts. In addition, in Figure 7, it is observed that at a temperature of 165 °C, the order parameter for ring I of PMAPHMB is 0.55. This compares favourably with the order parameter of 0.59 obtained for PMAPH at the corresponding reduced temperature of 125 °C. It is also observed in the Figure 7 that the range of order parameter values of both the mesogens in their nematic ranges are similar and typical of values observed generally for nematogenic mesogens. In the smectic A phase, PMAPHMB exhibits larger values of the order parameters. The slope of the plot in this phase is also marginally steeper than that in the nematic phase.

The dipolar coupling measurements at the specified temperatures provided the local order parameters of individual phenyl rings as listed in Table 3. The differences in the order parameters between different phenyl rings in the same molecule can be attributed to the rings being oriented at a small angle between them. The angle between the para-axes of the rings can be calculated from the values of  $S'_{zz}$  for the different rings by making the uniaxial approximation and by assuming that the long molecular axis is nearly parallel to para-axis of the phenyl ring with the largest order parameter. Thus values of angles between the para axes of rings III and II and rings II and I for the case of PMAPH have been obtained as 14.4° and 15.5° respectively. On the other hand, for PMAPHMB, the angle between the para-axes of adjacent rings starting from ring IV are 9.4°, 0° and 5.8°. The reduction in the angle between the different rings in this case compared to PMAPH can be interpreted as favoring a rod like molecular structure with the increase in the length of the core unit.

It is interesting to note that in the hydrogen bonded mesogen, the order parameter of the ring IV belonging to the benzoic acid moiety attached to the rest of the molecule through hydrogen bond and those of other phenyl rings connected between themselves via covalent bonds exhibit very similar local order parameters. This is akin to the behavior observed for systems with phenyl rings, all of which are connected by covalent

bonds.<sup>20</sup> This implies that in favorable cases, the hydrogen bonded molecules can replace covalent bonded systems, the advantages being ease of synthesis and the possibility of modulating the hydrogen bond and hence the property of the system.

In the present case, it is observed that the addition of the non-mesogenic acid to the mesogenic acceptor enhanced the phase and thermal stabilities of the latter and also induced an enantiotropic smectic A phase. The increase in the mesophase stability as well as the induction of smectic mesophase is expected as a consequence of the increase in molecular length for the hydrogen bonded mesogens and the presence of flexible terminal chains at both ends enhancing the aspect ratio. The interesting features observed in the present case with the incorporation of non-mesogenic donor indicate that the core length of mesogenic acceptor and the anisotropic polarizability have important role to play and that the presence of three phenyl rings in the core unit of acceptor meets the optimum requirements for the formation of the hydrogen bonded mesogenic material.

## Conclusions

A three ring based pyridine containing mesogenic acceptor was synthesized and mixed with non mesogenic 4-methoxy benzoic acid to get a hydrogen bonded complex. The formation of hydrogen bonding between acceptor and donor was confirmed by FT-IR spectroscopy where characteristic bands typical of hydrogen bonding of unionized type between pyridine and carboxylic acid was established. The presence of mesophases in the acceptor and the hydrogen bonded complex were evaluated by HOPM and DSC. Accordingly, the mesogenic acceptor showed a nematic phase whereas the hydrogen bonded complex exhibited both smectic A and nematic phases. <sup>13</sup>C NMR investigations in solution, solid state and nematic phase were in conformity with the expected molecular structure in different phases. In the nematic phase, the alignment of the mesogens in the magnetic field resulted in well resolved spectra. The spectral features in solution, solid state and liquid crystalline state indicated the presence of both acceptor and donor in the hydrogen bonded complex. The 2D SLF experiment provided <sup>13</sup>C-<sup>1</sup>H dipolar couplings which were used for computing the orientational order parameter. These values supported the rod-like nature for both acceptor and hydrogen bonded complex. The appearance of the smectic A phase and enhancement in the mesophase stability for the hydrogen bonded complex was on expected lines and can be attributed to an increase in the molecular length of the complex. The nearly identical order parameters obtained for all the phenyl rings in the complex is very similar to behavior observed for mesogens constructed only with covalent bonds and indicates that either of the approaches can be used. It may be emphasized that the H-bonded mesogens are relatively easier to synthesize and are also amenable to modifications giving rise to possibilities of creating a variety of different mesogenic systems. It may however be necessary that the realization of such complexes by incorporating non-mesogenic donor will require that the acceptor's core length is optimally designed.

## Acknowledgements

MKR and TNS sincerely thank Dr. A. B. Mandal, Director, CSIR-CLRI for his keen interest and constant support in this work. The partial financial support from NWP-23 is duly acknowledged. The use of the AV-III-500 Solid State NMR spectrometer funded by the Department of Science and Technology, New Delhi, at the NMR Research Centre, Indian Institute of Science, Bangalore, is gratefully acknowledged.

<sup>a</sup>Department of Chemistry, S.V. University, Tirupati 517 502, India. E-mails: kesavareddy2000@gmail.com and ksreddy01@rediffmail.com

<sup>b</sup>Polymer Laboratory, CSIR-Central Leather Research Institute, Adyar, Chennai 600 020, India. E-mail: tnswwamy99@hotmail.com

<sup>c</sup>Department of Physics, Indian Institute of Science, Bangalore 560012, India. E-mail: bibidasct@gmail.com

<sup>d</sup># Department of Physics, Indian Institute of Science, Bangalore 560012, India. Current address – Scientist Fellow, Chemical Physics Laboratory, CSIR-Central Leather Research Institute, Adyar, Chennai 600 020, India; E-mail: nitinlobo@gmail.com

<sup>e</sup>NMR Research Centre, Indian Institute of Science, Bangalore 560012, India. E-mail: kvr@sif.iisc.ernet.in

† Electronic Supplementary Information (ESI) available: [FT-IR spectra, solution 2D NMR data of PMAPHMB, SAMPI4 pulse sequence and DSC data]. See DOI: 10.1039/b000000x/

## References

- A.D. Demus in *Handbook of Liquid Crystals*, Vol.1 (Eds: D. Demus, J.W. Goodby, G.W. Gray, H.W. Spiess and V. Vill), WILEY-VCH, Weinhiem, Germany, 1998, p.133.
- G. W. Gray, *Molecular Structure and Properties of Liquid Crystals*, Academic Press: New York, 1962.
- G. R. Luckhurst and G. W. Gray, *The Molecular Physics of Liquid Crystals*; Academic Press: New York, 1979.
- T. Kato, N. Mizoshita and K. Kishimoto, *Angew. Chem., Int. Ed.*, 2006, **45**, 38.
- P. J. Collings and M. Hird, *Introduction to Liquid Crystals Chemistry and Physics*, Taylor and Francis, London, 1997.
- D. Demus, *Mol. Cryst. Liq. Cryst.*, 2001, **364**, 25.
- J. Etxebarria and M. Blanca Ros, *J. Mater. Chem.*, 2008, **18**, 2919.
- R. Amaranatha Reddy and C. Tschierske, *J. Mater. Chem.*, 2006, **16**, 907.
- K. Kato in *Handbook of Liquid Crystals*, Vol. 2B (Eds: D. Demus, J.W. Goodby, G.W. Gray, H.W. Spiess, V. Vill), WILEY-VCH, Weinhiem, Germany, 1998, p. 969.
- C. M. Palcos and D. Tsiourvas, *Liq. Cryst.*, 2001, **28**, 1127.
- T. Kato, *Struct. Bond.*, 2000, **96**, 95.
- T. Kato and J. M. J. Frechet, *Liq. Cryst.*, 2006, **33**, 1429.
- (a) M.R. Hammond and R. Mezzenga, *Soft Matter.*, 2008, **4**, 952. (b) J.M. Lehn, *Science.*, 2002, **295**, 2400.
- (a) W-T. Chuang, H-S. Sheu, U-S. Jeng, H-H. Wu, P-D. Hong and J-J. Lee, *Chem. Mater.*, 2009, **21**, 975. (b) M. Yoshio, Y. Shoji, Y. Tochigi, Y. Nishikawa and T. Kato, *J. Am. Chem. Soc.*, 2009, **131**, 6763. (c) J. Martinez-Perdiguero, Y. Zhang, C. Walker, J. Etxebarria, C.L. Folcia, J. Ortega, M. J. O'Callaghan and U. Baumeister, *J. Mater. Chem.*, 2010, **20**, 4905. (d) J.T. Korhonen, T. Verho, P. Rannou and O. Ikkala, *Macromolecules.*, 2010, **43**, 1507. (e) D. J. Broer, C. M. W. Bastiaansen, M. G. Debije and A. P. H. J. Schenning, *Angew. Chem. Int. Ed.*, 2012, **51**, 7102. (f) M. Roohnikan, M. brahimi, S. R. Ghaffarian and N. Tamaoki *Liq. Cryst.*, 2013, **40**, 314.
- T. Kato, *Supramol. Sci.*, 1996, **3**, 53.

- 16 J.W. Lee, J.-I. Jin, M. F. Achard and F. Hardouin, *Liq. Cryst.*, 2001, **28**, 663.
- 17 M. Pfaadt, G. Moessner, D. Pressner, S. Valiyaveetil, C. Boeffel, K. Mullen and H.W. Spiess, *J. Mater. Chem.*, 1995, **5**, 2265.
- 18 M. J. Duer, L. F. Gladden, A.C. Griffin, C. P. Jariwala and C. Stourton, *J. Chem. Soc., Faraday Trans.*, 1996, **92**, 803.
- 19 C. Tan and B. M. Fung, *J. Phys. Chem. B*, 2003, **107**, 5787.
- 20 (a) S. Kalaivani, T. Narasimhaswamy, B. Bibhuti Das, N. P. Lobo and K.V. Ramanathan, *J. Phys. Chem. B*, 2011, **115**, 11554. (b) T. Narasimhaswamy, D. K. Lee, K. Yamamoto, N. Somanathan and A. Ramamoorthy, *J. Am. Chem. Soc.*, 2005, **127**, 6958.
- 21 (a) A. Ramamoorthy, Ed. *Thermotropic Liquid Crystals: Recent Advances*; Springer: Dordrecht, The Netherlands, 2007. (b) R. Y. Dong, *Nuclear Magnetic Resonance Spectroscopy of Liquid Crystals*; World Scientific: Singapore, 2010.
- 22 (a) F. Perez, P. Judeinstein, J.P. Bayle, T. Brauniger and B. M. Fung, *New J. Chem.*, 1996, **20**, 1175. (b) F. Perez, J.P. Bayle and B. M. Fung, *New J. Chem.*, 1996, **20**, 537. (c) P. Berdague, F. Perez, J.P. Bayle, M.-S. Ho and B. M. Fung, *New J. Chem.*, 1995, **19**, 383. (d) J.P. Bayle, M.-S. Ho and B. M. Fung, *New J. Chem.*, 1993, **17**, 345.
- 23 M. Yoshiko, Y. Shoji, Y. Tochigi, Y. Nishikawa and T. Kato, *J. Am. Chem. Soc.*, 2009, **131**, 6763.
- 24 M. Prehm, F. Lin, Xiangbing, Zeng, G. Ungar and C. Tschirske, *J. Am. Chem. Soc.*, 2008, **130**, 14922.
- 25 C. Lavigneur, E. J. Foster and V. E. Williams, *J. Am. Chem. Soc.*, 2008, **130**, 11791.
- 26 J. Jensen, S.C. Grundy, S.L. Bretz and C.S. Hartley, *J. Chem. Educ.*, 2011, **88**, 1133.
- 27 B. Neises and W. Steglich, *Angew. Chem., Int. Ed.*, 1978, **17**, 522.
- 28 F.D. Bellamy and K. O. U., *Tetrahedron Lett.*, 1984, **25**, 839.
- 29 T. Kato and J. M. J. Frechet, *J. Am. Chem. Soc.*, 1989, **111**, 8533.
- 30 B. M. Fung, A. K. Khitrin and K. Ermolaev, *J. Magn. Reson.*, 2000, **142**, 97.
- 31 A. A. Nevzorov and S.J. Opella, *J. Magn. Reson.*, 2007, **185**, 59.
- 32 N. P. Lobo, M. Prakash, T. Narasimhaswamy and K.V. Ramanathan, *J. Phys. Chem. A*, 2012, **116**, 7508.
- 33 B. Bibhuti Das, T. G. Ajitkumar and K. V. Ramanathan, *Solid State NMR*, 2008, **33**, 57.
- 34 T. Narasimhaswamy and K.S.V. Srinivasan, *Liq. Cryst.*, 2004, **31**, 1457.
- 35 T. Kato, T. Uryu, F. Kaneuchi, C. Jin and J. M. J. Frechet, *Liq. Cryst.*, 1993, **14**, 1311.
- 36 J.Y. Lee, P. C. Painter and M. M. Coleman, *Macromolecules*, 1988, **21**, 346.
- 37 S. L. Johnson and K. A. Ruman, *J. Phys. Chem.*, 1965, **69**, 74.
- 38 S. E. Odinkov and A. V. Iogansen, *Spectrochim. Acta A*, 1972, **28**, 2343.
- 39 C. B. S. Pourcain, *J. Mater. Chem.*, 1999, **9**, 2727.
- 40 I. Dierking, *Textures of Liquid Crystals*. Wiley-VCH Verlag GmbH, Weinheim; 2003.
- 41 W. T. Dixon, *J. Chem. Phys.*, 1982, **77**, 1800.
- 42 R.Y. Dong, J. Xu, J. Zhang and C. A. Veracini, *Phys. Rev. E*, 2005, **72**, 061701.
- 43 V. Domenici, C.A. Veracini, V. Novotna and R.Y. Dong, *ChemPhysChem*, 2008, **9**, 556.
- 44 B. Das, S. Grande, W. Weissflog, A. Eremin, M.W. Schroder, G. Pelzl, S. Diele and H. Kresse, *Liq. Cryst.*, 2003, **30**, 529.
- 45 B.M. Fung, *Prog. Nucl. Magn. Reson. Spectrosc.*, 2002, **41**, 171.
- 46 K.V. Ramanathan and N. Sinha, in *Current Developments in Solid State NMR Spectroscopy*. Vol VIII, Eds. N. Mueller; P.K., Madhu, Springer, Wienheim 2003, **55**, 45.
- 47 C.H. Wu, A. Ramamoorthy and S.J. Opella, *J. Magn. Reson. A*, 1994, **109**, 270.
- 48 J. Xu, K. Fodor-Csorba and R.Y. Dong, *J. Phys. Chem. A*, 2005, **109**, 1998.
- 49 (a) C.S. Nagaraja and K.V. Ramanathan, *Liq. Cryst.*, 1999, **26**, 17. (b) Z. Gan, *J. Magn. Res.*, 2000, **143**, 136.
- 50 B.M. Fung, J. Afzal, T.L. Foss and M-H Chau, *J. Chem. Phys.*, 1986, **85**, 4808.
- 51 A. Marini and R.Y. Dong, *Phys. Rev. E*, 2011, **83**, 041712.
- 52 J. Zhang, V. Domenici and R.Y. Dong, *Chem. Phys. Lett.*, 2007, **441**, 237.

5

55

60

Table 1  $^{13}\text{C}$  NMR data of PMAPH in solution and liquid crystalline states. The chemical shifts have been referenced to tetramethylsilane at 0 ppm.

10

C.No	Solution (ppm)	Liquid Crystalline state (ppm) at 125 °C	AIS (ppm)	$^{13}\text{C}$ - $^1\text{H}$ Dipolar Oscillation Frequencies* (kHz) at 125 °C
1	163.6	219.8	56.2	1.55
2	114.3	138.2	23.9	2.33
3	132.3	160.7	28.4	2.28
4	121.3	179.2	57.9	1.51
5	164.9	205.5	40.6	-
6	148.3	210.2	61.9	1.59
7	122.0	144.3	22.3	2.49
8	122.6	149.4	26.8	2.56
9	150.1	215.5	65.4	1.50
10	157.9	197.1	39.2	4.03
11	142.7	210.2	67.5	1.79
12	122.2	149.4	27.2	2.56
13	150.6	166.6	16.0	1.81

15

20

\*For the dipolar oscillation frequencies, the errors are  $\pm 0.06$  kHz for protonated carbons and  $\pm 0.08$  kHz for quaternary carbons

85

25

90

30

95

35

100

40

105

45

110

50

115

120

50

5 **Table 2**  $^{13}\text{C}$  NMR data of PMAPHMB in solution and liquid crystalline states. The chemical shifts have been referenced to tetramethylsilane at 0 ppm.

55

10

15

20

25

C. No	Solution (ppm)	Liquid Crystalline state (ppm) at 130°C	AIS (ppm)	$^{13}\text{C}$ - $^1\text{H}$ Dipolar Oscillation Frequencies* (kHz) at 130°C
1	163.7	227.1	63.4	1.58
2	114.4	137.8	23.4	2.51
3	132.3	167.7	35.4	2.10
4	121.4	184.2	62.8	1.45
5	164.9	210.9	46.0	1.17
6	148.3	221.0	72.7	1.46
7	122.0	151.9	29.9	2.84
8	122.7	154.7	32.0	3.48
9	150.1	221.0	70.9	1.46
10	157.7	202.4	44.7	5.14
11	143.1	222.5	79.4	2.02
12	122.2	146.7	24.5	3.08
13	150.6	161.7	11.1	2.39
14	170.6	215.0	44.4	1.17
15	122.0	186.5	64.5	1.59
16	132.2	163.3	31.1	2.75
17	113.7	140.4	26.7	2.81
18	163.8	225.1	61.3	1.59

\*For the dipolar oscillation frequencies, the errors are  $\pm 0.06$  kHz for protonated carbons and  $\pm 0.08$  kHz for quaternary carbons.

100

30

105

35

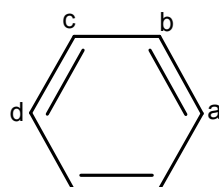
110

40

115

45

5 Table 3 Orientational Order Parameter values of PMAPH at 125 °C and PMAPHMB at 130 °C



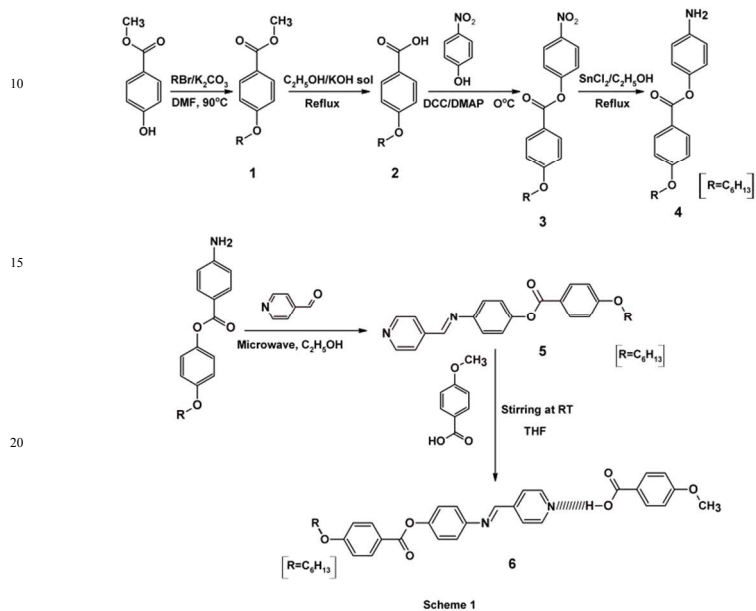
Mesogen	T (°C)	Ring	Angle		$S'_{zz}$	$S'_{xx}-S'_{yy}$	Calculated dipolar oscillation frequencies (kHz)			
			$\theta_b$	$\theta_c$			b	c	a*	d
PMAPH	125	I	120.6	120.8	0.59	0.058	2.34	2.28	1.37	1.38
		II	120.9	120.7	0.65	0.066	2.50	2.56	1.52	1.52
		III	119.2	122.0	0.58	0.043	2.56	1.85	1.78	-
PMAPHMB	130	I	120.6	122.0	0.64	0.058	2.5	2.11	1.48	1.51
		II	119.7	117.6	0.65	0.064	2.85	3.48	1.49	1.43
		III	118.9	121.2	0.65	0.062	3.07	2.39	2.01	-
		IV	120.5	120.3	0.68	0.069	2.74	2.81	1.58	1.58

\* For carbon *a* in ring III, the contribution of the azomethine proton has also been taken into account

**Figure Captions**

Scheme 1 Synthetic strategy for the target mesogens	60
5 Fig.1 Molecular Structures of (A) PMAPH and (B) PMAPHMB.	
Fig.2 HOPM photographs of mesogens while cooling from isotropic phase: (A) PMAPH nematic phase at 154 °C and (B) PMAPHMB – smectic A phase at 116 °C.	65
10	70
Fig.3 <sup>13</sup> C NMR spectra of PMAPH. Traces from bottom to top correspond respectively to spectra recorded in (A) solution, (B) solid state and (C) liquid crystalline phase at 125 °C.	75
15 Fig.4 Plots of <sup>13</sup> C chemical shifts for the aromatic carbons of (A) PMAPH and (B) PMAPHMB in their mesophases as a function of temperature. The corresponding carbon labels are indicated in the Figure.	80
Fig.5 2D SLF NMR spectra of (A) PMAPH at 125 °C in the nematic phase and (B) PMAPHMB at 130 °C in the nematic phase.	85
20	90
Fig.6 <sup>13</sup> C NMR spectra of PMAPHMB. Traces from bottom to top correspond respectively to spectra recorded in (A) solution, (B) solid state and (C) liquid crystalline phase at 130 °C.	90
25	
Fig. 7 Order parameters, S <sub>zz</sub> and S <sub>xx</sub> – S <sub>yy</sub> for ring-I of (A) PMAPH and (B) PMAPHMB in their mesophases as a function of temperature obtained by using the CSA values of 4-Hexyloxybenzoic acid (HBA) <sup>32</sup> .	95
30	100
35	105
40	110
45	115
50	120
55	125

5



Scheme 1

Scheme 1 Synthetic strategy for the target mesogens

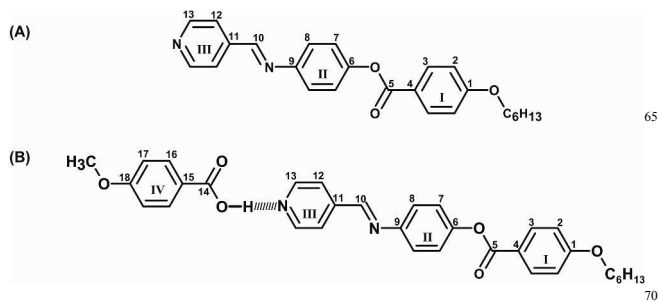


Fig. 1 Molecular Structures of (A) PMAPH and (B) PMAPHMB.

55

5

60

10

65

15

20

25

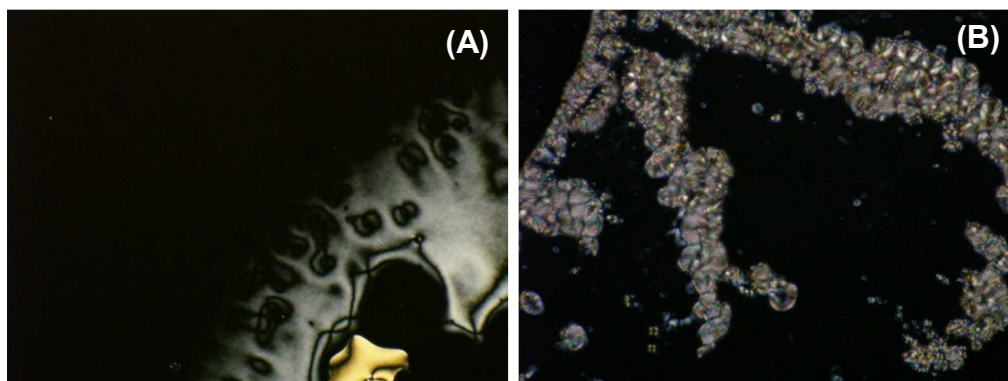


Fig.2 HOPM photographs of mesogens while cooling from isotropic phase: (A) PMAPH nematic phase at 154 °C and (B) PMAPHMB - smectic A phase at 116 °C.

30

35

40

45

50

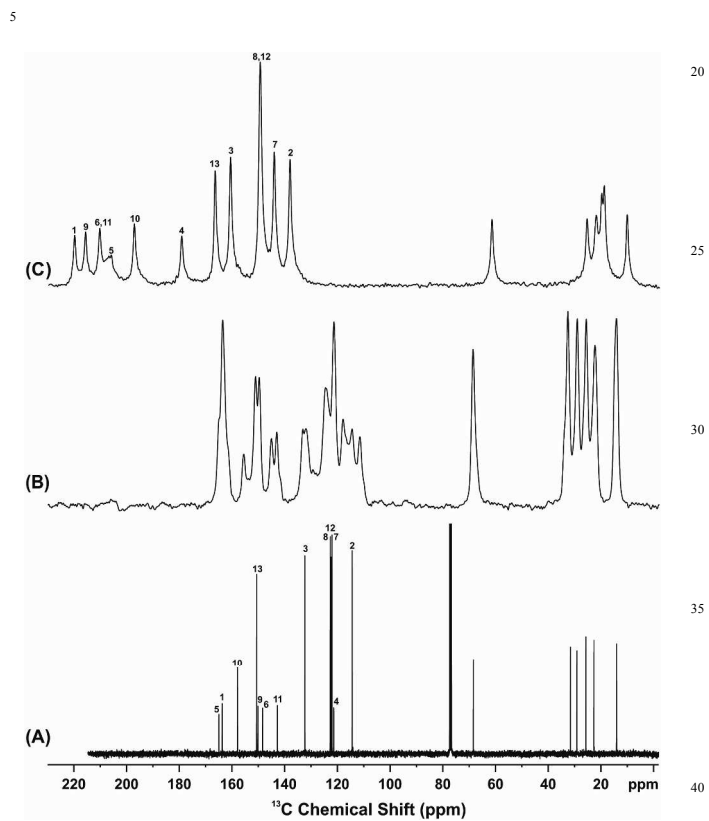


Fig. 3  $^{13}\text{C}$  NMR spectra of PMAFH. Traces from bottom to top correspond respectively to spectra recorded in (A) solution, (B) solid state and (C) liquid crystalline phase at 125 °C.

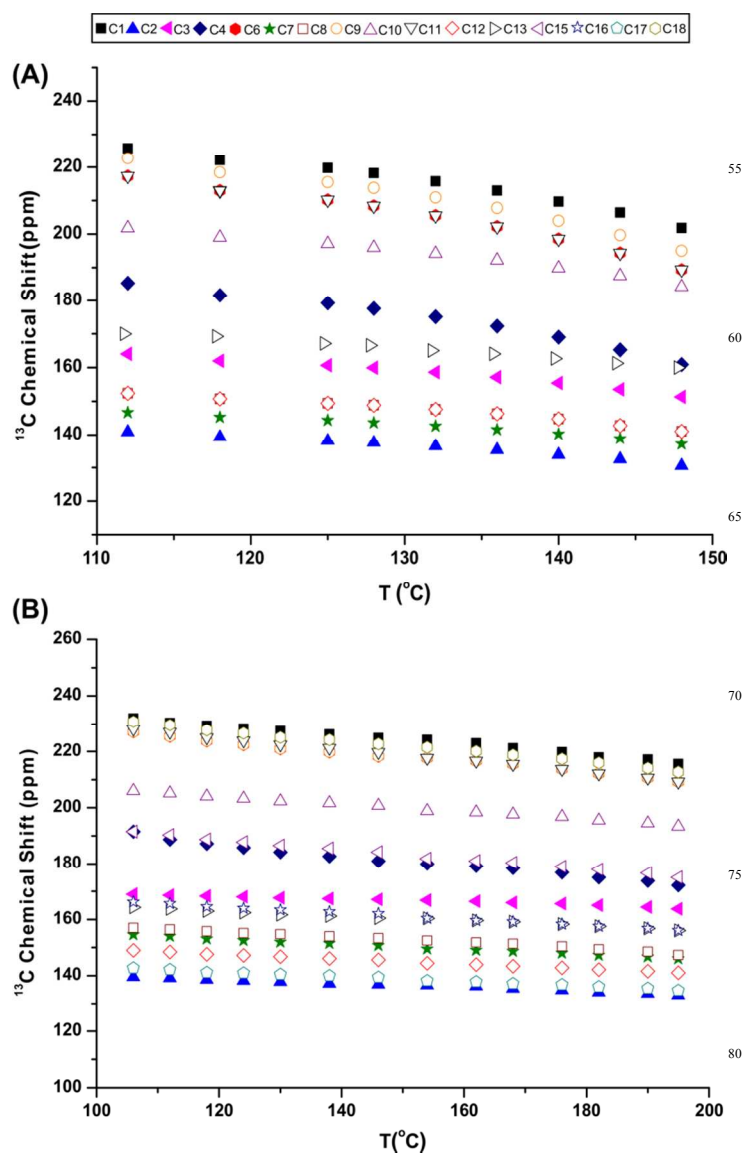
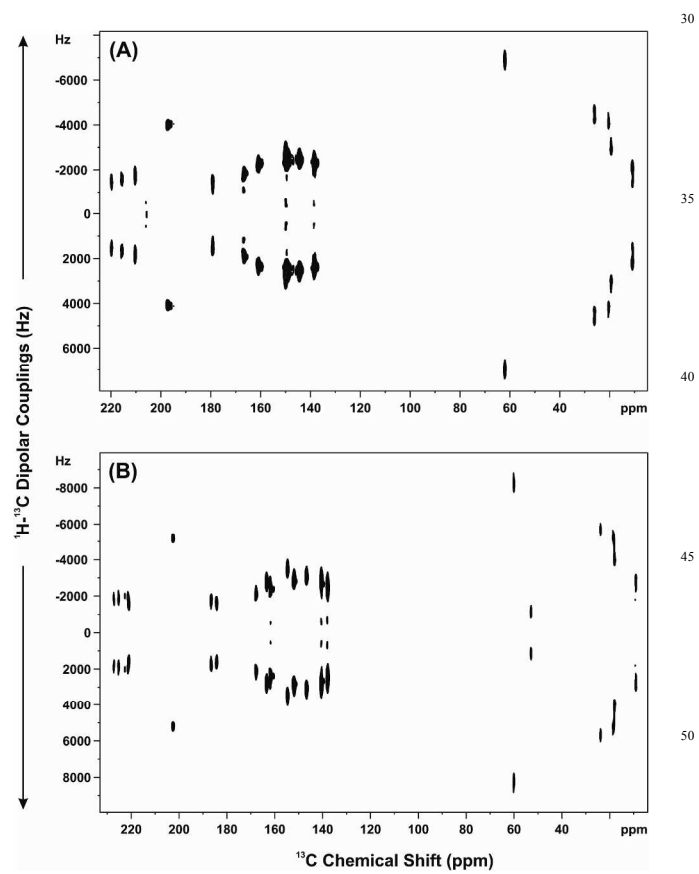


Fig.4 Plots of  $^{13}\text{C}$  chemical shifts for the aromatic carbons of (A) PMAFH  
and (B) PMAFHMB in their mesophases as a function of temperature.  
The corresponding carbon labels are indicated in the Figure.



5  
Fig.5 2D SLF NMR spectra of (A) PMAPH at 125 °C in the nematic phase and (B) PMAPHMB at 130 °C in the nematic phase.

10

15

20

25

30

35

40

45

50

55

60

65

70

75

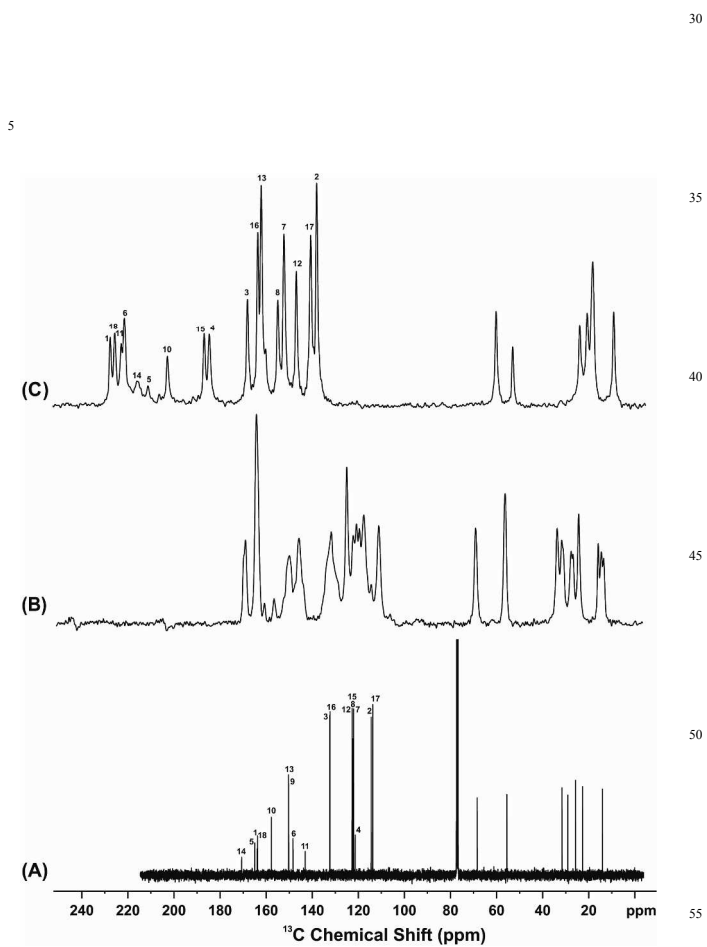
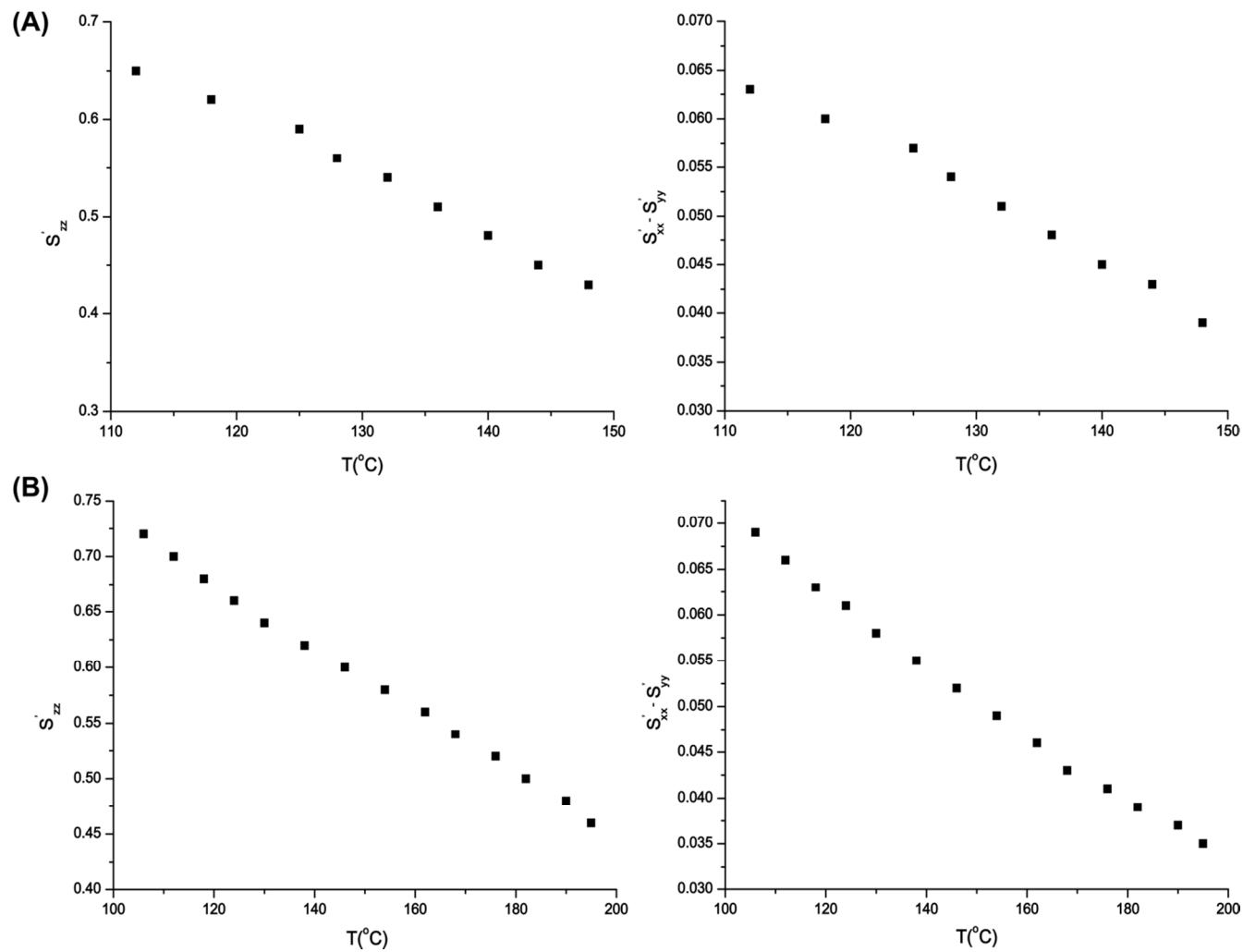


Fig. 6  $^{13}\text{C}$  NMR spectra of PMAHMB. Traces from bottom to top correspond respectively to spectra recorded in (A) solution, (B) solid state and (C) liquid crystalline phase at 130 °C.



5

25

Fig. 7 Order parameters,  $S'_{zz}$  and  $S'_{xx} - S'_{yy}$  for ring-I of (A) PMAPH and (B) PMAPHMB in their mesophases as a function of temperature  
10 obtained by using the CSA values of 4-Hexyloxybenzoic acid (HBA)<sup>32</sup>.

30

15

35

20